Published in final edited form as:
J Am Chem Soc. 2008 October 15; 130(41): 13673–13682. doi:10.1021/ja803612z.

A Mechanistic Study of Protein Phosphatase-1 (PP1), A Catalytically Promiscuous Enzyme

Claire McWhirter[†], **Elizabeth A. Lund**[§], **Eric A. Tanifum**[§], **Guoqiang Feng**[†], **Qaiser Sheikh**[†], **Alvan C. Hengge**[§], and **Nicholas H. Williams**[†]

§*Utah State University, Department of Chemistry and Biochemistry, Logan Utah 84322-0300, (alvan.hengge@usu.edu)*

†*University of Sheffield, Centre for Chemical Biology, Department of Chemistry, Sheffield, UK S3 7HF (N.H.Williams@Sheffield.ac.uk)*

Abstract

The reaction catalyzed by the protein phosphatase-1 (PP1) has been examined by linear free energy relationships and kinetic isotope effects. With the substrate 4-nitrophenyl phosphate (4NPP), the reaction exhibits a bell-shaped pH-rate profile for k_{cat}/K_M indicative of catalysis by both acidic and basic residues, with kinetic pK_as of 6.0 and 7.2. The enzymatic hydrolysis of a series of aryl monoester substrates yields a Brønsted β_{lg} of -0.32, considerably less negative than that of the uncatalyzed hydrolysis of monoester dianions (-1.23). Kinetic isotope effects in the leaving group with the substrate 4NPP are $^{18}(V/K)_{bridge}$ = 1.0170 and $^{15}(V/K)$ = 1.0010 which, compared against other enzymatic KIEs with and without general acid catalysis, are consistent with a loose transition state with partial neutralization of the leaving group. PP1 also efficiently catalyzes the hydrolysis of 4-nitrophenyl methylphosphonate (4NPMP). The enzymatic hydrolysis of a series of aryl methylphosphonate substrates yields a Brønsted β_{lg} of -0.30, smaller than the alkaline hydrolysis (-0.69) and similar to the β_{lg} measured for monoester substrates, indicative of similar transition states. The KIEs and the β_{lg} data point to a transition state for the alkaline hydrolysis of 4NPMP that is similar to that of diesters with the same leaving group. For the enzymatic reaction of 4NPMP, the KIEs are indicative of a transition state that is somewhat looser than the alkaline hydrolysis reaction, and similar to the PP1-catalyzed monoester reaction. The data cumulatively point to enzymatic transition states for aryl phosphate monoester and aryl methylphosphonate hydrolysis reactions that are much more similar to one another than the nonenzymatic hydrolysis reactions of the two substrates.

Introduction

Phosphoryl transfer reactions play fundamental roles in many biological processes, including metabolism, energy transduction, gene expression, and cell signaling. Protein phosphatase-1 (PP1) is a member of the phosphoprotein phosphatase (PPP) gene family, which is widely expressed in mammalian tissue and is critical for the control of many cellular pathways by antagonizing the effects of protein phosphorylation mediated by kinases. Four different catalytic subunit types of the protein phosphatases account for most of the phosphoserine/threonine phosphatase activity in eukaryotic cells (PP1, PP2A, PP2B and PP2C).[1] The catalytic subunits of the PPP family show high sequence homology, and the active sites of e.g. PP1,[2] PP2B[3] and PP5[4] are all very similar (although the control of these catalytic subunits depends

Supporting Information Available: Data analysis for calculation of kinetic isotope effects from isotope ratio data, and levels of isotopic incorporation into labeled substrates. This material is available free of charge via the Internet at http://pubs.acs.org.

on regulatory subunits in a complex interplay of inhibition and allosteric effects[5]). Highly conserved residues serve to bind two metal ions within ~3Å of each other, and further cationic residues (histidine and arginine) line the shallow depression on the surface to form the active site.[2] The two metal ions are held in octahedral coordination sites with a bridging hydroxyl and bridging acetate oxygen. Inorganic phosphate (product) or inhibitors (such as tungstate) form a 1,3 bridge between the two metal ions.[2] This active site geometry is also closely reflected in the purple acid phosphatases, which have the same metal ion coordination geometry at their active sites.[6] This suggests that a common mechanism may be applicable to these active sites which all catalyze phosphoryl transfer. Figure 1 depicts a diagram of the residues involved in coordination of the metal ions at the active site of PP1, and neighboring residues that may be involved in substrate binding and/or catalysis, from the X-ray structure.[7] The modeled phosphate monoester substrate is shown in a hypothetical binding mode.[7]

Uncatalyzed phosphoryl transfer reactions are extremely slow, but phosphatases can provide rate enhancements of $>10^{20}$-fold.[8] Enzyme-catalyzed phosphoryl transfer reactions have frequently been suggested to proceed through transition states that are altered from their solution counterparts, presumably as a result of interactions with active site catalytic groups such as metal ions. Characterizing the structure of the transition state is crucial to the understanding of how enzymes interact with and stabilize the transition state in order to provide the rate enhancements associated with biological catalysis.

A pictorial representation of the range of transition states for phosphoryl transfer is shown in the More-O'Ferrall Jencks diagram in Figure 2. In this diagram, bond fission is depicted on the horizontal coordinate and bond formation to the nucleophile on the vertical coordinate. A completely dissociative, two-step mechanism with metaphosphate intermediate would proceed through the lower right corner, but phosphoryl transfer reactions in aqueous solution do not form free metaphosphate as an intermediate.[9] The reactions of the dianions of phosphate monoesters are concerted, with loose transition states in which bond fission to the leaving group is extensive, but little bond formation to the nucleophile has occurred.[9,10] Such a transition state lies in the lower right-hand region of the diagram. Phosphodiesters with aryl leaving groups have been shown by linear free energy relationships[11,12] and kinetic isotope effects[13,14] to also react by a concerted pathway, although the transition state is tighter, in the central region of the diagram, in which bond fission to the leaving group is more synchronized with bond formation to the nucleophile. Phosphotriesters can react through an addition-elimination reaction that involves the phosphorane intermediate in the top left hand corner.

The catalytic subunit of protein phosphatase PP1 catalyzes the hydrolysis of phosphate monoesters. We have discovered that the hydrolysis of aryl methylphosphonates, which are diester analogues, is also efficiently catalyzed. This ability permits the analysis of two fundamental questions about catalysis. First, do the PP1-catalyzed reactions proceed by transition states that are the same as or altered from those of the uncatalyzed reactions? Secondly, do these two substrates, which normally react by different transition states, react by a similar transition state in their enzyme-catalyzed reactions? In order to address these questions, linear free energy relationship and kinetic isotope effect data have been obtained for the PP1-catalyzed reactions of both classes of substrates. These methods give different, complementary information about transition state structure. A comparison of the data obtained with the two substrate types to one another, as well as to their respective uncatalyzed hydrolyses, permits an evaluation of these questions. Figure 3 shows the aryl esters for which linear free energy relationship data were obtained, and the positions at which kinetic isotope effects were measured for the reactions of *p*-nitrophenyl phosphate (4NPP) and *p*-nitrophenyl methylphosphonate (4NPMP).

Results and Discussion

We expressed the catalytic subunit of PP1 (γ isoform, PP1γ) in *E. Coli* DH5a in the presence of 1 mM Mn(II) ions which are assumed to occupy the active site; previous reports with PP1α have established that Mn(II) is the most effective cofactor.[15] Initially, we needed to establish whether we could use steady state conditions to study the chemical step of the hydrolysis of aryl phosphates catalyzed by PP1γ. These studies were carried out using 4-nitrophenyl phosphate (4NPP) as substrate. Single turnover studies established that product release is not rate limiting as identical pseudo first order rate constants were obtained for 4NPP hydrolysis with excess (K_M>[E]≫[S]) and limiting (K_M>[S]≫[E]) PP1γ. The maximal value of k_{cat}/K_M is also well below the value of ~10^7 M^{-1} s^{-1} (see below) that would suggest the probability of a diffusion limited reaction. Viscosity studies confirmed this as no changes in the rate of 4NPP hydrolysis were observed when 20% sucrose or glycerol were used as viscosigens. Thus, the steady state parameters report on a rate limiting change in the enzyme-substrate complex, which we assign to the chemical step of the catalyzed reaction.

The pH dependence of k_{cat}/K_M was measured, and shows a bell-shaped profile (Figure **4a**). This was fit to equation 1, derived on the assumption that the active ionic form requires one acidic (defined by K_a^1 and one basic residue (defined by K_a^2, and revealed kinetic pK_as of 6.0 ±0.2 and 7.2±0.2 with a maximal rate of 1850±500 M^{-1} s^{-1}.

$$\frac{k_{cat}}{K_M}=\left(\frac{k_{cat}}{K_M}\right)_{max}\left(\frac{K_a^1[H^+]}{K_a^1K_a^2+K_a^1[H^+]+[H^+][H^+]}\right) \quad (1)$$

The lower pK_a is too high to be assigned to the deprotonation of the substrate (4NPP has pK_a = 5.0), and so these data indicate two titrating groups associated with the enzyme and that the substrate is bound in the dianion form. These can reasonably be assigned to metal bound water (potentially bridging the Mn(II) ions; 6.0) acting as a nucleophile and the conserved residue H125 (7.3; proposed as a general acid catalyst on the basis of structural data).[7,16] Small phosphates such as 4NPP are rather weakly binding substrates, and so separating the kinetic terms into k_{cat} and K_M data cannot be carried out reliably above ~pH 8 due to a steady increase in K_M with pH (and so above pH 8, the maximum concentration of substrate ≤ K_M). However, plotting k_{cat} up to pH 8 revealed that the ES complex has an ionizable group with pK_a 6.3±0.2. This is consistent with the assignment of the lower pK_a to metal bound hydroxide, representing a small perturbation due to the dianionic phosphate substrate coordinating to the metal ions. Inhibition by inorganic phosphate was measured to deduce the extent to which product accumulation can be tolerated without affecting the catalytic parameters; this is a severe problem in alkaline phosphatase studies, where K_i is ~1 μM.[17] For PP1γ, K_i was measured as 1.2±0.2 mM for inorganic phosphate at pH 8.0 (Figure **4b**) by fitting relative activity for 4NPP hydrolysis to equation 2 which describes competitive inhibition. This is in good agreement with the value of 1.6±0.9 mM previously reported using a tighter peptide binding substrate, where true competitive inhibition could be established.[18] Thus, we were readily able to measure initial rates of reaction without product inhibition by restricting substrate turnover to ≤0.1 mM.

$$\text{Relative activity}=\frac{v}{v_0}=\frac{K_i}{K_i+[P_i]} \quad (2)$$

We then assayed PP1γ with a range of substrates that had similar geometries but differing TS structures for functional group transfer. Sulfate and thiophosphate monoesters have transition states that lie close to the dissociative corner in Figure 1, whereas diesters and phosphonates (with good leaving groups) lie closer to the centre of the synchronous region with a more associative transition state. Using 4-nitrophenyl sulfate and 4-nitrophenyl thiophosphate, we observed little activity. On the other hand, we observed that using 4-nitrophenyl methyl

phosphate and 4-nitrophenyl methylphosphonate (4NPMP) significant activity could be observed at pH 8. In particular, PP1γ showed comparable activity to 4NPMP as for 4NPP at the same substrate concentration so we further characterized this phosphonate activity. The pH rate profile (Figure **4a**; fit to the same ionizations as for 4NPP), shows a maximal rate only ~10 fold less that that for 4NPP (240±30 M^{-1} s^{-1}), and we confirmed that the same K_i was observed for inhibition of this activity by inorganic phosphate as for the 4NPP reaction (Figure **4b**; independent fits to equation 2 are shown for both data sets).

In the substrate 4NPMP, one of the phosphoryl oxygens is replaced by a methyl group, thus minimizing the steric changes incurred; for the diester, the active site has to accommodate the addition of a methoxy group. Such promiscuity with closely matched substrates has been reported with alkaline phosphatase before, but is very much less effective than for the natural monoester substrates. Thus, alkaline phosphatase catalyses the hydrolysis of phosphate diesters or phosphonates with 4-nitrophenol leaving groups ~10^6 fold less rapidly than 4NPP.[19] PP1γ shows only a 10-fold decrease in activity in cleaving 4NPMP. However, it should also be noted that the background reactivity of both substrates must be taken into account to assess this similarity in the catalyzed reactions; it is the rate acceleration that provides the measure of catalytic proficiency. For the water catalyzed reaction of 4NPMP, the pseudo-first order rate constant at 25 °C is 1×10^{-9} s^{-1},[20] which is about the same (see figure 5b) as for the dianion of 4NPP (2×10^{-9} s^{-1}),[8,21] and so the proficiency of the enzyme for catalyzing both processes is very similar. The second order rate constant for hydrolysis of 4NPMP by hydroxide at 25 °C is 1.2×10^{-5} M^{-1} s^{-1} (see below) implying that the hydroxide dependent rate of reaction at pH 8 would be ~1×10^{-11} s^{-1}, significantly slower than the spontaneous reaction. If we make an estimate for the hydrolysis reaction that takes into account the pK_a of the nucleophile in the active site (6.0; see above) by interpolating between the second order rate constants for water and hydroxide attack (which gives an estimate for β_{nuc} of ~0.33), we arrive at an estimate of 7×10^{-9} M^{-1} s^{-1} for the reaction of 4NPMP with a nucleophile that has this pK_a.

To further characterize these reactions, we measured the linear free energy relationships (LFER) between the rate of the catalyzed reaction and the nature of the leaving group. A wide range of aryl phosphate monoesters were synthesized and used to measure Michaelis-Menten curves in triplicate, from which the ratio k_{cat}/K_M could be accurately measured for each substrate. The high values of K_M (~20-30 mM in each case) limited the level of enzyme saturation that we could obtain without varying the concentrations of different salts in our solutions substantially. In this situation, when the maximum substrate concentration used corresponds to relatively low levels of saturation, the individual values for k_{cat} and K_M obtained from the curve fits are much less accurately defined than their ratio. The pK_as of the phenols were measured under our experimental conditions by UV-Vis titration and these data used to construct a Brønsted plot (Figure **5a**). Using the k_{cat}/K_M parameter means that the plot reflects the change in charge at the departing oxygen from the ground state ester in solution to the transition state bound to the enzyme. This can be compared to the analogous plot for the solution reaction, which reports on the change in charge from the same starting state to the transition state in bulk solution. The slope of this plot (β = -0.32±0.03) is greatly reduced compared to the solution behavior of the monoester dianions (β = -1.23). In both cases, this parameter needs to be compared to the effect of these same perturbations on the equilibrium constant for the reaction (where β = -1.35) to be interpreted in terms of degree of reaction progress; in this case, through the fractional effective charge change on the leaving group in the transition state. For the solution reaction, this suggests a very advanced transition state with respect to leaving group departure, with ~91% effective charge change in the transition state.

We also synthesized a range of aryl methylphosphonates and measured the β value for the leaving groups for both the hydroxide promoted and PP1γ catalyzed hydrolysis reactions (Figure 5a and 5b). For the hydroxide reaction, β = -0.69±0.02; interpretation of this datum

also must take into account the equilibrium β value. Assuming a similar initial effective charge to a phosphate diester (where β_{eq} ~-1.74) indicates a much earlier TS (40% change in effective charge) than for the hydrolysis of monoester dianions in solution. This is likely to be an underestimate, as the methyl group should induce a smaller initial charge on the bridging oxygen than the methoxy group (β_{eq} decreases from 1.4 for transfer of a diphenylphosphate group to 1.25 for diphenylphosphinate transfer;[22] but is unlikely to be significantly removed from ~50% change in effective charge. However, for the PP1γ catalyzed reaction, β = -0.30 ±0.04 which is very similar to the sensitivity shown by the monoester substrates. Performing the same analysis would suggest that the transition state has become even earlier; alternatively, the similar low sensitivity to the leaving groups could indicate substantial charge neutralization within the active site, plausibly by a histidine residue acting as a general acid.

To complement the Brønsted data and further interrogate the potential bond cleavage/charge changes happening at the transition state, we measured heavy atom kinetic isotope effects for both types of substrate. Figure 3 shows the positions at which kinetic isotope effects were measured for both the solution hydrolyses of *p*-nitrophenyl phosphate (4NPP) and *p*-nitrophenyl methylphosphonate (4NPMP), and for the PP1-catalyzed hydrolyses.

The magnitude of ^{15}k ($^{15}(V/K)$ in an enzymatic reaction) reflects the negative charge developed on the leaving group in the transition state, and arises from contributions of a quinonoid resonance structure in the delocalized nitrophenolate anion.[22-24] This secondary KIE attains a maximum value of ~ 1.0030 when the nitrophenolate group bears a full charge in the transition state. The leaving group ^{18}O KIE ($^{18}k_{lg}$) is a measure of P-O bond fission. The magnitude of this primary isotope effect is proportional to bond fission in the transition state, and with the nitrophenyl leaving group, values as large as 1.035 have been measured[23]; in a general acid-assisted reaction, the magnitude is reduced by protonation which has an inverse effect. Changes in P-O bonding in the phosphoryl group are reflected in $^{18}k_{nonbridge}$; loss of a pi bond to form a phosphorane results in a normal $^{18}k_{nonbridge}$, while a metaphosphate-like transition state exhibits a slight inverse effect. Data with alkaline phosphatase have shown that coordination to a metal center can result in a small inverse $^{18}(V/K)$ as a result of stiffening or restriction of bending and torsional modes.[25]

Table 2 shows the combined KIE and LFER results for the uncatalyzed hydrolysis reactions and for the PP1-catalyzed reactions of both substrates. The slow rate of the uncatalyzed monoester reaction required that these KIEs be measured at 95° C. The elevated temperature suppresses the magnitude of the KIEs by approximately 20%, which is insufficient to change the interpretation of the results presented here. As the phosphonate reaction is hydroxide catalyzed, the faster rate at high pH conditions allowed this reaction to be performed at 25°C. All KIEs were determined triplicate experiments. From each experiment, the KIE was calculated independently from measurements of the isotope ratio in recovered product, and, from the ratio in residual substrate, as described in the Experimental section. The independent calculation of each isotope effect using both measurements also provided an internal check of the results. The KIEs calculated from isotope ratios in product and from residual substrate agreed within experimental error in all cases, and the six values were averaged together to give the results in Table 2.

Due to the presence in PP1 of a histidine residue that is proposed to act as a general acid, for purposes of comparison, Table 2 includes previously reported data for protein-tyrosine phosphatases (PTPs), which utilize a conserved aspartic acid general acid in catalysis. These enzymes are well characterized, exhibit rate-limiting chemistry, and the KIEs for both the native reaction and for general acid mutants have been reported.[26,27,30] These data give expected ranges of values for the KIEs when the scissile oxygen atom is protonated during catalysis, and when it is not. In the former case, since the leaving group is neutralized, $^{15}(V/$

K) is unity, and $^{18}(V/K)$ is approximately 1.015 when P-O bond fission is extensive. When acid catalysis is lost in the Asp to Asn mutants, the leaving group departs as a nitrophenolate anion and the late transition state results in leaving group KIEs near their maximum values. The highly charged leaving group results in normal values of $^{15}(V/K)$ close to 1.0030, and the removal of the inverse contribution from protonation leads to larger $^{18}(V/K)_{bridge}$ values of 1.0275 - 1.0297.

It is reasonable to ask whether the weakly basic 4-nitrophenyl leaving group would require protonation in the transition state. In PTP-catalyzed reactions, loss of the general acid results in rate reductions of from two to three orders of magnitude when assayed with 4NPP, in addition to the changes in KIEs, indicating the importance of acid catalysis even with this leaving group. Within the confines of the active site, the departing anion may become protonated or else significantly stabilized through hydrogen bonding even if the product phenol is anionic when finally released into solution.

Results for PP1-catalyzed reaction of 4NPP

The degree of bond cleavage implied by the β_{lg} value of -0.32 depends upon the choice of the β value for the equilibrium reaction. Normalizing this data with the known β value for the equilibrium reaction of the dianion in solution (-1.35) leads to an estimate of about 23% bond cleavage, which is much retarded compared to the uncatalyzed case (91% bond cleavage) - making the assumption that change in effective charge can be equated to bond cleavage. This indicates that in the transition state of the PP1-catalysed reaction, there is either much reduced bond cleavage, or else charge quenching. A reaction where leaving group departure is catalyzed by proton transfer should be relatively insensitive to the pK_a of the leaving group as bond cleavage is compensated for by the catalytic interaction. If the leaving group is protonated in the transition state, then the relevant β_{eq} value is that representing the difference in effective charge between the reactant dianion and neutral phenol (-0.35). In this case, the observed β indicates a much larger degree of bond cleavage (91%), essentially the same as for the dianion reaction in solution.

Like the Brønsted β_{lg} values, the KIEs in the leaving group for the PP1-catalyzed reaction of 4NPP are diminished from their values in the uncatalyzed hydrolysis. Both results indicate less charge on the leaving group in the transition state of the PP1-catalyzed reaction. This could arise from a more diester-like transition state that is more associative, with less P-O bond fission. However, transition states for diester hydrolyses typically result in much smaller magnitudes for the primary $^{18}k_{lg}$ and in normal nonbridging ^{18}O KIEs.[23] Instead, the magnitude of $^{18}(V/K)_{nonbridge}$ for 4NPP is slightly more inverse than in the uncatalyzed reaction. This suggests that the reduction in β_{lg} and the leaving group KIEs results instead from partial neutralization by an enzymatic group. This could be accomplished either by coordination of the scissile oxygen atom with a metal ion, or by protonation. The binding mode of substrates to the active site of PP1 is generally assumed to involve coordination of the phosphoryl group to the metal center, either monodentately or in a bidentate fashion. This would make coordination of the leaving group to one of the metal ions unlikely. Neutralization of the leaving group in PP1 and related enzymes is proposed to occur by means of a conserved histidine residue, H125 in PP1.[7,16] Site directed mutants of H125 are not readily expressed; the small amounts of H125S and H125A that have been obtained are inactive, and in our hands no detectable activity for 4NPP hydrolysis could be observed with the H125A mutant.[16] This observation is consistent with the hypothesized role of H125 as a general acid, though the effect on protein expression provokes suspicion of potential structural consequences of the mutation. The data indicate that charge neutralization is not complete; the $^{15}(V/K)$ indicates the presence of about a third of a negative charge on the leaving group, and the observation of a significant β_{lg} also rules out complete neutralization. Complete neutralization would result in a set of KIEs

and a β_{lg} similar to those for reactions of the native PTPs (Table 2). The overall picture supported by the data is a transition state with extensive P-O bond fission, in which general acid catalysis is involved, but in which proton transfer lags somewhat behind P-O bond fission. This results in a small partial negative charge on the leaving group, as indicated by the modest values for $^{15}(V/K)$ and $\beta_{LG.}$

The $^{18}(V/K)_{nonbridge}$ is more inverse than that observed either in the uncatalyzed reaction of 4NPP dianion, or in the PTP-catalyzed reactions. This KIE is slightly inverse in metaphosphate-like transition states, and becomes successively more normal in the progressively tighter transition states of diesters and triesters. In addition to bonding changes in the transition state, this isotope effect may also be affected by interactions with metal ions. If coordination to the metal center stiffens bending modes, or introduces new vibrational modes, inverse contributions can arise. Coordination of oxygen to divalent metal ions has been demonstrated to give rise to inverse isotope effects in solution[31] and in enzymatic reactions.[32] Vibrational spectroscopy has demonstrated that metal ion coordination to phosphoryl oxygen atoms can significantly affect the frequencies of vibrational modes.[33] This effect is not general. For example, no significant isotope effect was observed for coordination of Mg^{2+} to inorganic phosphate in solution.[34] Very small inverse isotope effects are observed for coordination to calcium in solution,[35] and very small inverse values of $^{18}(V/K)_{nonbridge}$ were observed with λ protein phosphatase containing Mn^{2+} or Ca^{2+} in the active site.[35] In contrast, the alkaline phosphatase-catalyzed (the R166S mutant, for which chemistry is rate-limiting) hydrolysis of an aryl and alkyl phosphate monoester substrate results in values of $^{18}(V/K)_{nonbridge}$ that are significantly more inverse (0.9925 and 0.9933 respectively) than in the uncatalyzed hydrolysis reactions of the same compounds (0.9994 and ~1.00).[36] Similarly, inverse values for $^{18}(V/K)_{nonbridge}$ are observed for the calcineurincatalyzed hydrolysis of 4NPP with Mn^{+2} (0.9942) or Mg^{2+} (0.9910) at the active site.[37] Based on these precedents, it seems reasonable to attribute the inverse nonbridge KIE observed for the PP1-catalyzed reaction to coordination to the metal center. Whether such binding is monodentate or bidentate, bridging the two metals, cannot be determined from the data.

Results for 4NPMP reactions

In contrast to phosphate and phosphinate esters, which have been subjected to considerable mechanistic study, the reactions of phosphonates do not seem to have been examined in detail. The linear free energy and kinetic isotope effect data presented here seems to be the first such data presented for this class of compounds. It seems logical to draw comparisons between the methylphosphonates examined here and the isoelectronic phosphate diesters.

The Brønsted β_{lg} obtained for the alkaline hydrolysis of a series of aryl methylphosphonates is -0.69 (Table 2). This is modestly larger than the reported value of -0.64 for the alkaline hydrolysis of a similar set of aryl methyl phosphate diesters under identical conditions,[38] but slightly smaller than the value of -0.94 recently obtained from data measured at 42 °C.[39] The same value has been observed for the reaction of phenoxide with aryl methyl phosphate diesters.[11] The reactivity of the compounds is about an order of magnitude greater than the corresponding diesters. As it is likely that the effect of the methyl for methoxy substitution is to reduce the initial effective charge on the bridging oxygen, a slightly lower value for the β_{lg} would still reflect a similar change in the bonding between the P and O in the transition state. The $^{18}k_{bridge}$ for the alkaline hydrolysis of 4NPMP is slightly larger than the range of values reported for several diesters with the *p*-nitrophenyl leaving group.[23] The magnitude of $^{18}k_{nonbridge}$ is somewhat smaller, indicative of less associative character, and more synchronous nucleophilic bond formation and leaving group bond fission. The presence of significant isotope effects in both the nucleophile and the leaving group describe the alkaline hydrolysis of diesters as concerted.[13] The similar LFER and KIE data suggest that the

hydrolysis of 4NPMP is most likely concerted as well, though with some modest differences in transition state structure.

The KIE and LFER data for the PP1-catalyzed reaction of 4NPMP both differ from the data for the alkaline hydrolysis. The β_{lg} of -0.30 is significantly reduced, and is not significantly different from the value for the PP1-catalyzed reaction of the monoester substrate. The leaving group isotope effects are both greater in the PP1 reaction, and while P-O bond fission inferred from the $^{18}(V/K)_{bridge}$ of 1.0170 is not as large as that for the monoester substrate, it is significantly larger than that for the alkaline hydrolysis.

The small and inverse $^{18}(V/K)_{nonbridge}$ for the PP1-catlayzed reaction of 4NPMP presumably also arises from coordination to the metal center. The difference in this KIE between the catalyzed and uncatalyzed reactions is larger for 4NPMP than for 4NPP, whether one looks at the overall isotope effect or at the per-atom value. Such a difference could result from a change to a slightly more dissociative transition state; alternatively, the stiffening of bending and torsional modes resulting from coordination to the metal center may be more pronounced for the methylphosphonate substrate than for the monoester. These values argue against a more associative transition state for the PP1-catalyzed reaction resulting from metal ion coordination.

Conclusions

These data imply that the transition states of the PP1-catalyzed reactions of the two substrates are much more similar to one another than the transition states of the respective uncatalyzed reactions. For the monoester substrate 4NPP, the transition state implied by the KIEs in the enzymatic and the uncatalyzed reactions are similar, with both characterized by extensive leaving group bond fission, and little nucleophilic participation. The reduction in magnitude of the Brønsted β_{lg} most likely reflects partial charge neutralization by a general acid, as also reflected in the modest $^{15}(V/K)$. The phosphonate substrate 4NPMP undergoes hydroxide promoted hydrolysis by a mechanism and transition state similar to that of phosphate diesters, though with slightly greater P-O bond fission. The PP1-catalyzed hydrolysis of 4NPMP shows modest differences in the KIEs that indicate a larger extent of bond fission, closer to that of the monoester reaction. A reduced β_{lg} most likely reflects general acid catalysis, as in the monoester reaction. The modest inverse nonbridge KIEs on the PP1-catalyzed hydrolysis of both substrates most likely result from binding interactions with the metal center. This interpretation suggests that catalysis of 4NPMP hydrolysis in the active site of PP1γ is achieved by a distortion of the solution transition state structure, but with minimal energetic penalty as the catalytic proficiency for hydrolyzing both processes is rather similar.

Materials and Methods

Synthesis of Aryl methylphosphonates

Synthesis of Diaryl methylphosphonates (Scheme 1)

Diaryl methylphosphonates were prepared by the following procedure exemplified by preparation of diphenyl methylphosphonate. Methyl phosphonodichloride (1.50 g, 11 mmol) and phenol (2.14 g, 22 mmol) were dissolved in 20 mL of dry dichloromethane. The mixture was cooled in an ice-water bath. Triethylamine (4.45g, 44mmol) in dry dichloromethane (5 mL) was then added dropwise to the cool mixture while stirring and white precipitate was formed. After addition was finished, the mixture was stirred for another 3 hours at room temperature. The reaction mixture was poured into 20 mL cold water, and the resulting solution was extracted with dichloromethane. The combined dichloromethane layer was dried over

Na_2SO_4. Removal of the solvent yielded the crude diphenyl methylphosphonate. The crude product was purified by a short silica column to afford a viscous oil, 2.65g, 94%.

Bis(*p*-nitro-*m*-fluorophenyl) methylphosphonate—pale yellow solid, 40% yield, ^{1}H NMR (250 MHz, $CDCl_3$) δ/ppm 8.11 (m, 2H, Ar-H), 7.15-7.25 (m, 4H, Ar-H), 1.97 (d, *J* = 17.70 Hz, 3H, CH_3). ^{31}P NMR (101 MHz, $CDCl_3$) δ/ppm 26.24. MS (EI+) 374 (M^+). HR-MS calculated for $C_{13}H_9F_2N_2O_7P$ 374.0115, found 374.0103.

Bis(*p*-nitrophenyl) methylphosphonate—pale yellow solid, 93% yield, ^{1}H NMR (250 MHz, $CDCl_3$) δ/ppm 8.23 (d, *J* = 9.16 Hz, 4H, Ar-H), 7.36 (dd, *J* = 9.15 and 1.22 Hz, 4H, Ar-H), 1.95 (d, *J* = 18.01 Hz, 3H, CH_3). ^{13}C NMR (63 MHz, $CDCl_3$) δ/ppm 154.60 (d, *J* = 8.58 Hz, 2C), 145.11 (2C), 125.87 (4C), 121.06 (d, *J* = 4.77 Hz, 4C), 12.12 (d, *J* = 145.91 Hz, CH_3). ^{31}P NMR (101 MHz, $CDCl_3$) δ/ppm 25.52. MS (EI+) 338 (M^+, 100%). HR-MS calculated for $C_{13}H_{11}N_2O_7P$ 338.0303, found 338.0290.

Bis(*m*-nitrophenyl) methylphosphonate—colorless oil, 85% yield, ^{1}H NMR (250 MHz, $CDCl_3$) δ/ppm 7.97-8.04 (m, 4H, Ar-H), 7.44-7.56 (m, 4H, Ar-H), 1.90 (d, *J* = 17.70 Hz, 3H, CH_3). ^{13}C NMR (63 MHz, $CDCl_3$) δ/ppm 150.22 (d, *J* = 8.59 Hz, 2C), 149.00 (2C), 130.72 (2C), 126.80 (d, *J* = 3.81 Hz, 2C), 120.53 (2C), 116.06 (d, *J* = 4.76 Hz, 2C), 11.97 (d, *J* = 144.96 Hz, CH_3). ^{31}P NMR (101 MHz, $CDCl_3$) δ/ppm 26.20. MS (EI+) 338 (M^+, 100%). HR-MS calculated for $C_{13}H_{11}N_2O_7P$ 338.0303, found 338.0289.

Bis(*p*-chlorophenyl) methylphosphonate—white solid, 97% yield, ^{1}H NMR (250 MHz, $CDCl_3$) δ/ppm 7.29 (dd, *J* = 2.14 and 8.85 Hz, 4H, Ar-H), 7.11 (dd, *J* = 1.22 and 8.85 Hz, 4H, Ar-H), 1.80 (d, *J* = 17.70 Hz, 3H, CH_3). ^{13}C NMR (63 MHz, $CDCl_3$) δ/ppm 148.63 (d, *J* = 8.59 Hz, 2C), 130.79 (2C), 129.89 (4C), 121.83 (d, *J* = 4.77 Hz, 4C), 11.59 (d, *J* = 144.96 Hz, CH_3). ^{31}P NMR (101 MHz, $CDCl_3$) δ/ppm 24.97. MS (EI+) 316 (M^+, 100%). HR-MS calculated for $C_{13}H_{11}Cl_2O_3P$ 315.9822, found 315.9834.

Bis(*m*-chlorophenyl) methylphosphonate—colorless oil, 85% yield,^{1}H NMR (250 MHz, $CDCl_3$) δ/ppm 7.15-7.28 (m, 6H, Ar-H), 7.06-7.12 (m, 2H, Ar-H), 1.81 (d, *J* = 17.70 Hz, 3H, CH_3). ^{13}C NMR (63 MHz, $CDCl_3$) δ/ppm 150.51 (d, *J* = 7.63 Hz, 2C), 135.12 (2C), 130.61 (2C), 125.75 (2C), 121.13 (d, *J* = 4.77 Hz, 2C), 118.82 (d, *J* = 3.82 Hz, 2C), 11.66 (d, *J* = 144.96 Hz, CH_3). ^{31}P NMR (101 MHz, $CDCl_3$) δ/ppm 24.83. MS (EI+) 316 (M^+, 100%). HR-MS calculated for $C_{13}H_{11}Cl_2O_3P$ 315.9822, found 315.9837.

Bis(*p*-methylphenyl) methylphosphonate—white solid, 99% yield, ^{1}H NMR (250 MHz, $CDCl_3$) δ/ppm 7.11 (d, *J* = 8.85 Hz, 4H, Ar-H), 7.06 (d, *J* = 8.85 Hz, 4H, Ar-H), 2.30 (s, 6H, $PhCH_3$), 1.74 (d, *J* = 17.71 Hz, 3H, CH_3). ^{13}C NMR (63 MHz, $CDCl_3$) δ/ppm 148.12 (d, *J* = 8.58 Hz, 2C), 134.76 (2C), 130.26 (4C), 120.24 (d, *J* = 3.81 Hz, 4C), 20.72 ($2CH_3$), 11.32 (d, *J* = 144.01 Hz, CH_3). ^{31}P NMR (101 MHz, $CDCl_3$) δ/ppm 24.40. MS (EI+) 276 (M^+, 100%). HR-MS calculated for $C_{15}H_{17}O_3P$ 276.0915, found 276.0911.

Bisphenyl methylphosphonate—colorless oil, 94% yield, ^{1}H NMR (250 MHz, $CDCl_3$) δ/ppm 7.29-7.35 (m, 4H, Ar-H), 7.13-7.21 (m, 6H, Ar-H), 1.78 (d, *J* = 17.70 Hz, 3H, CH_3). ^{13}C NMR (63 MHz, $CDCl_3$) δ/ppm 150.28 (d, *J* = 7.63 Hz, 2C), 129.86 (4C), 125.25 (2C), 120.55 (d, *J* = 3.82 Hz, 4C), 11.54 (d, *J* = 144.96 Hz, CH_3). ^{31}P NMR (101 MHz, $CDCl_3$) δ/ppm 24.29. MS (EI+) 248 (M^+). HR-MS calculated for $C_{13}H_{13}O_3P$ 248.0602, found 248.0594.

Synthesis of aryl methylphosphonate sodium salts (Scheme 1)

Aryl methylphosphonates were prepared by the following procedure exemplified by preparation of phenyl methylphosphonate. A mixture of diphenyl methylphosphonate (2.46 g, 10 mmol) in 44 mL of NaOH (0.3 M) was heated to reflux until the oil layer of diphenyl methylphosphonate was no longer visible (about 30 min). The solution was rapidly cooled, neutralized to pH 7 with HCl, and extracted with dichloromethane to remove the phenol. The aqueous phase was then strongly acidified by adding HCl and extracted with dichloromethane. The dichloromethane layer was dried over Na_2SO_4. Removal of the solvent yielded the crude phenyl methylphosphonic acid as a viscous oil, 1.60 g, 94%. This was then was converted (quantitatively) to the sodium salt by shaking in one equivalent of sodium methoxide in methanol.

***p*-nitro-*m*-fluorophenyl methylphosphonate—**pale yellow solid, ^{1}H NMR (250 MHz, D_2O) δ/ppm 8.17 (m, 1H, Ar-H), 7.10-7.20 (m, 2H, Ar-H), 1.46 (d, *J* = 16.79 Hz, 3H, CH_3). ^{31}P NMR (101 MHz, D_2O) δ/ppm 25.96. TOF MS (ES+) 280 (M + Na^+). HR-MS calculated for $C_7H_6FNO_5Na_2P$ (M + Na^+) 279.9763, found 279.9756.

p-nitrophenyl methylphosphonate—pale yellow solid, ^{1}H NMR (250 MHz, D_2O) δ/ppm 8.21 (d, *J* = 9.16 Hz, 2H, Ar-H), 7.28 (m, *J* = 9.16 Hz, 2H, Ar-H), 1.46 (d, *J* = 16.79 Hz, 3H, CH3). ^{13}C NMR (63 MHz, D_2O) δ/ppm 157.54, 143.46, 125.89 (2C), 121.29 (2C), 12.37 (d, *J* = 139.23 Hz, CH_3). ^{31}P NMR (101 MHz, D_2O) δ/ppm 25.59. TOF MS (ES+) 262 (M + Na^+). HR-MS calculated for $C_7H_7NO_5Na_2P$ (M + Na^+) 261.9857, found 261.9853.

***m*-nitrophenyl methylphosphonate—**white solid, ^{1}H NMR (250 MHz, D_2O) δ/ppm 7.97-8.03 (m, 2H, Ar-H), 7.50-7.59 (m, 2H, Ar-H), 1.44 (d, *J* = 16.78 Hz, 3H, CH).^{13}C NMR (63 MHz, D_2O) δ/ppm 152.16, 148.57, 130.57, 128.01, 119.24, 116.20, 12.10 (d, *J* = 138.29 Hz, CH_3). ^{31}p NMR (101 MHz, D_2O) δ/ppm 25.87. TOF MS (ES+) 262 (M + Na^+). HR-MS calculated for $C_7H_7NO_5Na_2P$ (M + Na^+) 261.9857, found 261.9870.

***p*-chlorophenyl methylphosphonate—**white solid, ^{1}H NMR (250 MHz, D_2O) δ/ppm 7.35 (d, *J* = 8.85 Hz, 2H, Ar-H), 7.09 (m, *J* = 8.85 Hz, 2H, Ar-H), 1.38 (d, *J* = 16.48 Hz, 3H, CH_3). ^{13}C NMR (63 MHz, D_2O) δ/ppm 150.25, 129.60 (2C), 128.86, 122.56 (2C), 12.00 (d, *J* = 138.28 Hz, CH_3). ^{31}P NMR (101 MHz, D_2O) δ/ppm 25.49. TOF MS (ES+) 251 (M + Na^+). HR-MS calculated for $C_7H_7ClO_3Na_2P$ (M + Na^+) 250.9617, found 250.9626.

***m*-chlorophenyl methylphosphonate—**white solid, ^{1}H NMR (250 MHz, D_2O) δ/ppm 7.32 (m, 1H, Ar-H), 7.17-7.20 (m, 2H, Ar-H), 7.05-7.09 (m, 1H, Ar-H), 1.39 (d, *J* = 16.48 Hz, 3H, CH_3). ^{13}C NMR (63 MHz, D_2O) δ/ppm 152.23, 134.13, 130.75, 124.41, 121.42, 119.62, 12.05 (d, *J* = 138.28 Hz, CH_3). ^{31}P NMR (101 MHz, D_2O) δ/ppm 25.54. TOF MS (ES+) 251 (M + Na^+). HRMS calculated for $C_7H_7O_3Na_2PCl$ (M + Na^+) 250.9617, found 250.9613.

***p*-methylphenyl methylphosphonate—**white solid, ^{1}H NMR (250 MHz, D_2O) δ/ppm 7.19 (d, *J* = 8.24 Hz, 2H, Ar-H), 7.02 (m, *J* = 8.24 Hz, 2H, Ar-H), 2.28 (s, 3H, $PhCH_3$), 1.36 (d, *J* = 16.48 Hz, 3H, CH_3).^{13}C NMR (63 MHz, D_2O) δ/ppm 149.22, 134.34, 130.18 (2C), 120.94 (2C), 19.85, 11.94 (d, *J* = 138.29 Hz, CH_3).^{31}P NMR (101 MHz, D_2O) δ/ppm 25.34. TOF MS (ES+) 231 (M + Na^+), 209 (M + H^+). HR-MS calculated for $C_8H_{10}O_3NaP$ (M + H^+) 209.0344, found 209.0334.

phenyl methylphosphonate—white solid, ^{1}H NMR (250 MHz, D_2O) δ/ppm 7.38 (m, 2H, Ar-H), 7.14-7.22 (m, 3H, Ar-H), 1.40 (d, *J* = 16.48 Hz, 3H, CH_3).^{13}C NMR (63 MHz, D_2O) δ/ppm 151.64, 129.88 (2C), 124.43, 121.19, 121.13, 12.1 (d, *J* = 138.29 Hz, CH_3).^{31}P NMR

(101 MHz, D_2O) δ/ppm 25.35. TOF MS (ES+) 217 ($M + Na^+$), 195 ($M + H^+$). HR-MS calculated for $C_7H_8O_3Na_2P$ ($M + Na^+$) 217.0006, found 217.0009.

Kinetic methods

For the hydrolysis of the methyl arylphosphonates, the reactions were monitored by initial rate measurements using UV/Vis spectroscopy to measure the appearance of phenolate in 0.1 M NaOH. For 4NPMP, first order behavior in both substrate and hydroxide were confirmed at 25 °C. For the less reactive substrates, data was gathered at several temperatures between 90 and 40°C and extrapolated to 25 °C using an Arrhenius plot. The pK_a of each phenol was measured at 25 °C by monitoring the change in absorbance due to the phenolate with changing pH. For the PP1γ catalyzed reactions, reactions were initiated by addition of enzyme to an equilibrated mixture of substrate at 25 °C (I = 0.45M, NaCl; 100 mM AMPD buffer; 1mM $MnCl_2$) For the reactions involving phenols with a 4-nitro substituent, reactions could be monitored by the appearance of the product phenolate using UV/Vis spectroscopy (410 nm). For the other leaving groups, reactions were monitored either by quenching aliquots in strong base and monitoring the increase in absorbance of the phenolate, or through HPLC analysis of the reaction mixtures.

Synthesis of isotopically labeled substrates

The ^{15}N isotope effect was measured using natural abundance 4NPP, synthesized from *p*nitrophenol.[40] [^{14}N]-*p*-nitrophenol and [^{15}N]-*p*-nitrophen-[^{18}O]ol were synthesized as previously described.[28] After mixing to closely reconstitute the natural abundance of ^{15}N, this mixture was then phosphorylated[40] to produce *p*-nitrophenyl phosphate as a mixture of isotopomers. This mixture was used for determination of the $^{18}O_{lg}$ isotope effect. For measurement of the nonbridging oxygen isotope effect, [^{14}N]-*p*-nitrophenyl phosphate and [^{15}N]-*p*-nitrophenyl-[$^{18}O_3$]-phosphate were synthesized,[28] and mixed.

Natural abundance*p*-nitrophenyl methylphosphonate—(4NPMP) was prepared according to the method described above for aryl methylphosphonates.

^{18}O-methylphosphonic acid (Scheme 2)—To a solution of imidazole (2.54 g, 65.1 mmol) in dry THF (60 mL) under nitrogen, was added dichloromethylphosphine (500 μL, 5.43 mmol) slowly to form a white suspension. The mixture was then cooled to 0°C followed by addition of iodine (3.20 g, 10.9 mmol). The resulting brown solution was stirred for 30 min after which ^{18}O-labeled water (1.00 g, 50.0 mmol) was added and allowed to stir overnight at room temperature. The THF was then stripped *in vacuo* and the resulting dark-brown residue dissolved in water and extracted thoroughly with diethyl ether to obtain a clear aqueous phase. Silver nitrate (1.84 g, 10.8 mmol) was added to precipitate soluble iodide. Following filtration of the resulting yellow precipitate, the filtrate was passed through a sodium ion exchange column and subsequently through DOWEX® (50 WX) resin. The resulting solution was freeze-dried to obtain the ^{18}O-labeled acid as a pale-yellow sticky solid (390 mg, 75 % yield). ^1H NMR (300 MHz, dioxane-D_8) δ/ppm 7.62 (s, 2H, OH), 1.38 (d, J = 19.12 Hz, 3H, CH_3); ^{13}C NMR (75 MHz, dioxane-D_8) δ/ppm 11.81 (d, J = 123.01 Hz,); ^{31}P NMR (121 MHz, dioxane-D_8) δ/ppm 32.10.

$^{18}O_2$-Nonbridge,^{15}N-*p*-nitrophenyl methylphosphonate (Scheme 2)—^{18}O-labeled methylphosphonic acid (102 mg, 1.00 mmol), ^{15}N-labeled *p*-nitrophenol (426 mg, 3.00 mmol), trichloroacetonitrile (433 mg, 3.00 mmol), and imidazole (408 mg, 6.00 mmol) were dissolved in freshly distilled acetonitrile and heated at 70°C for 72 h, after which the reaction was judged complete by ^{31}P NMR. It was then concentrated *in vacuo* and the ensuing yellow paste dissolved in water, titrated down to pH 4.0 and extracted with diethyl ether to recover unreacted *p*-nitrophenol. The aqueous layer was then passed through a sodium ion exchange column,

followed by successive recrystallizations in acetone/ethanol mixtures to obtain the sodium salt of the $^{18}O_2$-Nonbridge,^{15}N-*p*-nitrophenyl methylphosphonate as a white powder (130 mg, 53% yield). ^{1}H NMR (300 MHz, D_2O) δ/ppm 8.16 (d, *J* = 9.20 Hz, 2H, Ar-H), 7.20 (d, *J* = 9.20 Hz, 2H, Ar-H), 1.35 (d, *J* = 19.41 Hz, 3H, CH_3); ^{13}C NMR (75 MHz, D_2O) δ/ppm 157.48, 143.38, 125.82 (2C), 121.23, 121.18, 12.29 (d, *J* = 137.67 Hz,); ^{31}P NMR (121 MHz, D_2O) δ/ppm 25.76: HR-MS calculated for $C_7H_7{}^{15}NO_3{}^{18}O_2P$ (M^+) 221.1014, found 221.0121 (73% $^{18}O_2$-nonbridge with the rest singly ^{18}O-labeled).

^{14}N-bis(*p*-nitrophenyl) methylphosphonate—Prepared as described in the general synthesis of bisaryl methylphosphonates using ^{14}N-labeled nitrophenol.

Pale yellow solid; 95% yield; ^{1}H NMR (300 MHz, $CDCl_3$) δ/ppm 8.24 (d, *J* = 10.32 Hz, 2H, Ar-H), 7.36 (d, *J* = 10.32 Hz, 2H, Ar-H), 1.94 (d, *J* = 17.85 Hz, 3H, CH_3); ^{13}C NMR (75 MHz, $CDCl_3$) δ/ppm 154.76, 154.65, 145.16 (2C), 125.96 (4C), 121.20 (2C), 121.13 (2C), 12.20 (d, *J* = 144.12 Hz,); ^{31}P NMR (121 MHz, $CDCl_3$) δ/ppm 25.81.

^{14}N-*p*-nitrophenyl methylphosphonate—Prepared as described in the general synthesis of aryl methylphosphonates, from ^{14}N-labeled bis(*p*-nitrophenyl) methylphosphonate.

^{18}O-Bridge,^{15}N-*p*-nitrophenyl methylphosphonate—Prepared as described in the general synthesis of aryl methylphosphonates using ^{18}O-labeled, ^{15}N-labeled *p*-nitrophenol.

Natural abundance *p*-nitrophenyl methylphosphonate—Prepared as described in the general synthesis of aryl methylphosphonates. White solid; 80% yield; ^{1}H NMR (300 MHz, D_2O) δ/ppm 8.17 (d, *J* = 9.62 Hz, 2H, Ar-H), 7.20 (d, *J* = 9.62 Hz, 2H, Ar-H), 1.35 (d, *J* = 18.10 Hz, 3H, CH_3); ^{13}C NMR (75 MHz, D_2O) δ/ppm 157.47, 143.45, 125.8 (2C), 121.25, 121.20, 12.20 (d, *J* = 138.39 Hz,); ^{31}P NMR (121 MHz, D_2O) δ/ppm 25.76.

Isotope Effect Measurements

All isotope effect measurements were performed in triplicate. Each reaction was carried to partial completion, and the hydrolyzed *p*-nitrophenol was extracted with ether. The residual substrate was then completely hydrolyzed and the resulting *p*-nitrophenol was similarly extracted. After purification by sublimation, all *p*-nitrophenol samples were analyzed by isotope ratio mass spectrometry to determine their nitrogen isotopic ratios. Each isotope effect experiment gives two independent determinations of the isotope effect, one from the isotope ratio in the product, the other from the isotope ratio in the residual substrate. From the isotopic ratios in the original reactant (R_o), in product (R_p) and in residual substrate (R_s), fractions of reaction, and degree of isotopic incorporation, the KIEs were calculated using equations 3 and 4.[41]

$$\text{isotope effect}=\log(1-f)/\log\left(1-f\left(R_p/R_o\right)\right) \quad (3)$$

$$\text{isotope effect}=\log(1-f)/\log\left[(1-f)\left(R_s/R_o\right)\right] \quad (4)$$

The ^{15}N isotope effects were measured using natural abundance substrate. The ^{18}O KIEs were measured using the remote label method[23] with the double-labeled substrates described above. The observed isotope effects from experiments to determine ^{18}O KIEs were corrected for the ^{15}N effect and for incomplete levels of isotopic incorporation in the substrate.[42]

Alkaline hydrolysis of *p*-nitrophenyl methylphosphonate

For the chemical hydrolysis of *p*-nitrophenyl methylphosphonate, 100 μmol was partially hydrolyzed in 25 mL of 1 N NaOH at 25°C. The half-life of this reaction is approximately 9

hours, and varying reaction times gave fractions of reaction ranging from 40-70%. The progress of the reaction was monitored by observing the formation of *p*-nitrophenol by UV-Visible spectroscopy at 400 nm. For the absorbance measurements, 25μL of the reaction solution was diluted in 3 mL of 0.1 N NaOH.

When 4NPMP was hydrolyzed to the desired fraction of reaction, a 500 μL aliquot was set aside for measuring the fraction of reaction. Then, the remaining solution was immediately titrated with HCl to pH 3.5, both protonating the p-nitrophenol for extraction and halting the alkaline hydrolysis. The *p*-nitrophenol was then extracted with diethyl ether (3×25 mL). The ether extracts were dried over magnesium sulfate and concentrated to dryness by rotary evaporation. Then the remaining aqueous solution was titrated back up to 1 N in hydroxide with NaOH and remaining 4NPMP was hydrolyzed completely at 50°C for at least 13 hours (the half-life for the hydrolysis of 4NPMP at 50°C is approximately 1 hour). The aliquot of the original reaction solution was also heated at 50°C for at least 13 hours, and the final absorbance was obtained in the same manner as previously described. The fraction of reaction is the ratio of the initial absorbance of the solution to the final absorbance after complete hydrolysis.

PP1-catalyzed hydrolysis of *p*-nitrophenyl methylphosphonate

The PP1-catalyzed reactions were run at 25°C in a freshly prepared buffer solution containing 100 mM TRIS pH 7.0, with 150 mM NaCl, 1 mM $MnCl_2$, and 1 mM DTT. Sufficient enzyme, from 20-35 μL of 30 μM human PP-1, was added to partially hydrolyze 100 μmol of each substrate in 5 mL of buffer, with the fraction of reaction ranging from 40-70%. For the 4NPMP, the catalyzed half-life at 25°C is approximately 12 hours, with enzyme activity decreasing over time. The progress of reaction was monitored by measuring the absorbance at 400 nm of a 5 μL of the reaction solution diluted in 3 mL of 0.1 N NaOH.

When 4NPMP was hydrolyzed to the desired fraction of reaction, two 100 μL aliquots of the solution were set aside to determine the fraction of reaction. The first was diluted in 400 μL of pH 4 acetate buffer. The second aliquot was diluted in 400 μL of 1 N NaOH and heated at 50°C for at least 13 hours. Immediately after the aliquots were removed and diluted, the enzymatic reaction mixture was titrated to pH 3.5, halting PP1-catlayzed hydrolysis. The nitrophenol was extracted, and the remaining substrate in the aqueous layer was then completely hydrolyzed as described for the total hydrolysis of residual substrate in the alkaline hydrolysis reaction. The concentrations of *p*-nitrophenol were determined in the two 500 μL aliquots, from the absorbance at 400 nm of a dilution of 25 μL in 3 mL of 0.1 NaOH. The fraction of reaction is the ratio of the absorbance of the initial aliquot, measured just after dilution, to the final absorbance reading of the completely hydrolyzed aliquot.

PP1-catalyzed hydrolysis of *p*-nitrophenyl phosphate—These reactions were carried out as described for 4NPMP, except for the method used to hydrolyze remaining substrate in the aqueous layer after partial reaction. For 4NPP the residual substrate was titrated to pH 9 in TRIS buffer, and commercial alkaline phosphatase was added. The reaction was allowed to proceed for 12 hours to insure complete hydrolysis of remaining 4NPP. Similarly, for the aliquots removed for determination of the fraction of reaction, the second aliquot was diluted in 400 μL of pH 9 TRIS buffer, and alkaline phosphatase was added to completely hydrolyze the substrate before assay at 400 nm.

Supplementary Material

Refer to Web version on PubMed Central for supplementary material.

Acknowledgment

This work was supported by a grant from the National Institutes of Health to ACH (GM47297) and by a grant from the Biology and Biotechnology Science Research Council to NHW (C18734). EAL thanks the Willard L. Eccles Foundation for an undergraduate research fellowship.

References

(1). Takai A, Mieskes G. The Biochemical journal 1991;275(Pt 1):233–9. [PubMed: 1850239]

(2). Egloff M, Cohen PT, Reinemer P, Barford D. J. Mol. Biol 1995;254:942–959. [PubMed: 7500362]

(3). Kissinger CR, Parge HE, Knighton DR, Lewis CT, Pelletier LA, Tempczyk A, Kalish VJ, Tucker KD, Showalter RE, Moomaw EW, et al. Nature 1995;378:641–4. [PubMed: 8524402]

(4). Swingle MR, Honkanen RE, Ciszak EM. The Journal of biological chemistry 2004;279:33992–9. [PubMed: 15155720]

(5). Johnson DF, Moorhead G, Caudwell FB, Cohen P, Chen YH, Chen MX, Cohen PT. European journal of biochemistry / FEBS 1996;239:317–25. [PubMed: 8706735]

(6). Sträter N, Klabunde T, Tucker P, Witzel H, Krebs B. Science (New York, N.Y 1995;268:1489–1492.

(7). Goldberg J, Huang HB, Kwon YG, Greengard P, Nairn AC, Kuriyan J. Nature 1995;376:745–753. [PubMed: 7651533]

(8). Lad C, Williams NH, Wolfenden R. Proc. Natl. Acad. Sci. U. S. A 2003;100:5607–10. [PubMed: 12721374]

(9). Herschlag D, Jencks WP. J. Am. Chem. Soc 1989;111:7579–7586.

(10). Thatcher GRJ, Kluger R. Adv. Phys. Org. Chem 1989;25:99–265.Hengge, AC. Comprehensive Biological Catalysis: A Mechanistic Reference. Sinnott, M., editor. Vol. 1. Academic Press; San Diego, CA: 1998. p. 517-542.

(11). Ba-Saif SA, Davis AM, Williams A. J. Org. Chem 1989;54:5483–5486.

(12). Kirby AJ, Younas M. J. Chem. Soc. (B) 1970:1165–1172.

(13). Cassano AG, Anderson VE, Harris ME. J. Am. Chem. Soc 2002;124:10964–10965. [PubMed: 12224928]

(14). Hengge AC, Tobin AE, Cleland WW. J. Am. Chem. Soc 1995;117:5919–5926.

(15). Huang HB, Horiuchi A, Goldberg J, Greengard P, Nairn AC. Proc. Natl. Acad. Sci. U. S. A 1997;94:3530–5. [PubMed: 9108010]

(16). Zhang J, Zhang Z, Brew K, Lee EY. Biochemistry 1996;35:6276–82. [PubMed: 8639569]

(17). O'Brien PJ, Herschlag D. Biochemistry 2002;41:3207–25. [PubMed: 11863460]

(18). Sanvoisin J, Pollard JR, Hormozdiari WH, Ward J, Gani D. J. Chem. Soc., Perkin Trans. I 2001:1709–1715.

(19). O'Brien PJ, Herschlag D. Biochemistry 2001;40:5691–9. [PubMed: 11341834]

(20). Behrman EJ, Biallas MJ, Brass HJ, Edwards JO, Isaks M. J. Org. Chem 1970;35:3063–3069.

(21). Kirby AJ, Varvoglis AG. J. Am. Chem. Soc 1967;89:415–423.

(22). Ba-Saif SA, Waring MA, Williams A. J. Am. Chem. Soc 1990;112:8115–8120.Bourne N, Chrystiuk E, Davis AM, Williams A. J. Am. Chem. Soc 1988;110:1890–1895.

(23). Hengge AC. Acc. Chem. Res 2002;35:105–12. [PubMed: 11851388]

(24). Hengge AC, Cleland WW. J. Am. Chem. Soc 1990;112:7421–7422.

(25). Catrina I, O'Brien P J, Purcell J, Nikolic-Hughes I, Zalatan JG, Hengge AC, Herschlag D. J Am Chem Soc. 2007

(26). Hengge AC, Sowa GA, Wu L, Zhang Z-Y. Biochemistry 1995;34:13982–13987. [PubMed: 7577995]

(27). Hengge AC, Denu JM, Dixon JE. Biochemistry 1996;35:7084–7092. [PubMed: 8679534]

(28). Hengge AC, Edens WA, Elsing H. J. Am. Chem. Soc 1994;116:5045–5049.

(29). Zhang Z-Y, Malochowski WP, Van Etten RL, Dixon JE. J. Biol. Chem 1994;269:8140–8145. [PubMed: 8132539]Zhang ZY, Wu L, Chen L. Biochemistry 1995;34:16088–96. [PubMed: 8519766]

(30). Hengge AC, Zhao Y, Wu L, Zhang Z-Y. Biochemistry 1997;36:7928–7936. [PubMed: 9201938]
(31). Feder HM, Taube H. J. Chem. Phys 1952;20:1335–1336.Taube H. J. Phys. Chem 1954;58:523–528.
(32). Cassano AG, Anderson VE, Harris ME. Biochemistry 2004;43:10547–10559. [PubMed: 15301552]
(33). de la Fuente M, Hernanz A, Navarro R. J. Biol. Inorg. Chem 2004;9:973–986. [PubMed: 15452776] Koleva VG. Spectrochim. Acta A 2007;66:413–418.Stangret J, Savoie R. Can. J. Chem 1992;70:2875–2883.
(34). Jones JP, Weiss PM, Cleland WW. Biochemistry 1991;30:3634–3639. [PubMed: 2015221]
(35). Hoff RH, Mertz P, Rusnak F, Hengge AC. J. Am. Chem. Soc 1999;121:6382–6390.
(36). Zalatan JG, Catrina I, Mitchell R, Grzyska PK, O'Brien P,J, Herschlag D, Hengge AC. J Am Chem Soc 2007;129:9789–98. [PubMed: 17630738]
(37). Hengge AC, Martin BL. Biochemistry 1997;36:10185–10191. [PubMed: 9254616]Martin BL, Jurado LA, Hengge AC. Biochemistry 1999;38:3386–92. [PubMed: 10079083]
(38). Williams NH, Cheung W, Chin J. J. Am. Chem. Soc 1998;120:8079–8087.
(39). Zalatan JG, Herschlag D. J Am Chem Soc 2006;128:1293–303. [PubMed: 16433548]
(40). Bourne N, Williams A. J. Org. Chem 1984;49:1200–1204.
(41). Bigeleisen J, Wolfsberg M. Adv. Chem. Phys 1958;1:15–76.
(42). Cleland, WW. Isotope effects in chemistry and biology. Kohen, A.; Limbach, H-H., editors. CRC Press; Boca Raton, FL: 2006. p. 915-930.

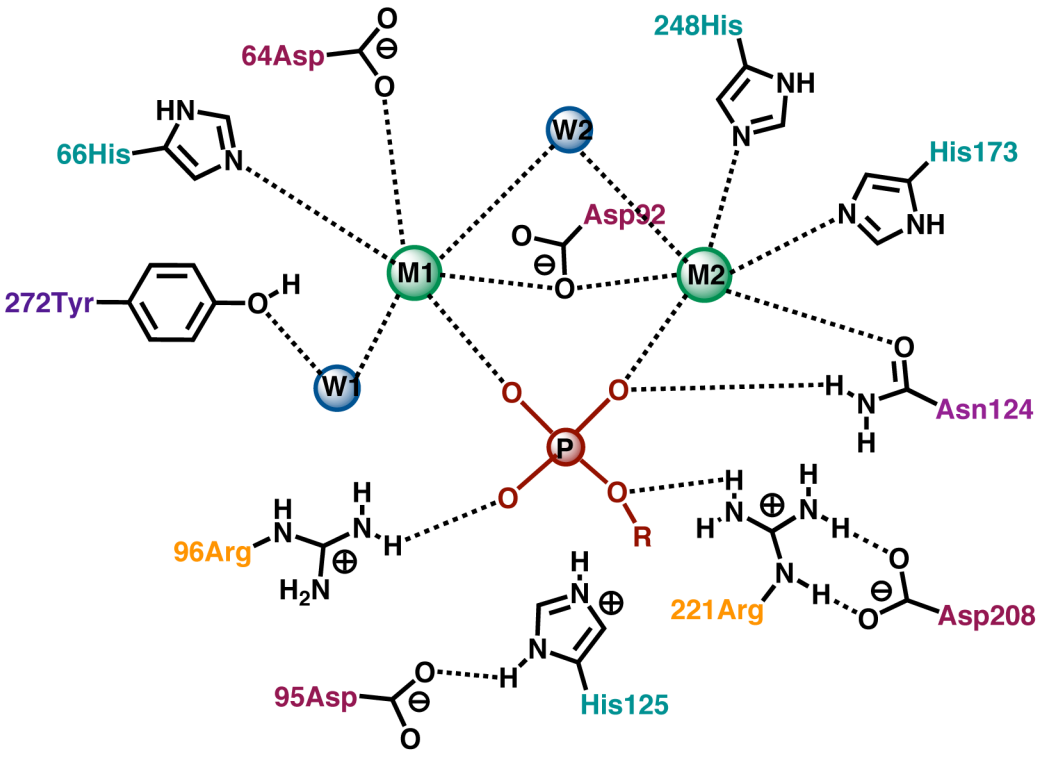

Figure 1.
A schematic diagram of the active site of PP1 showing a substrate modeled in a hypothetical binding mode.[7]

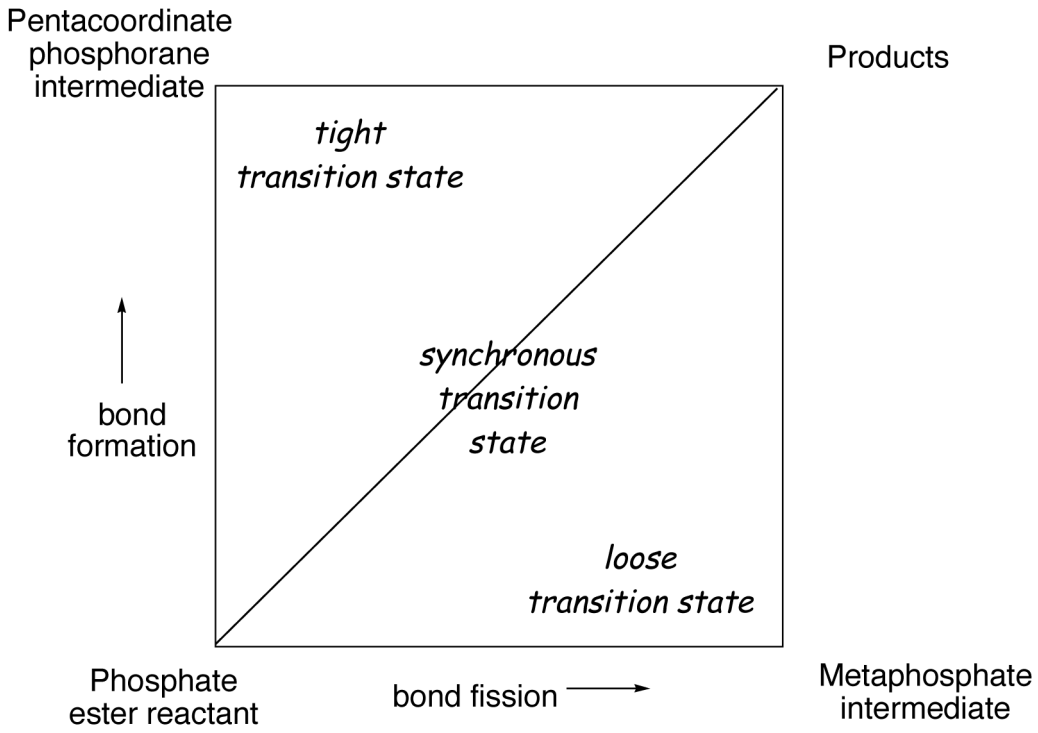

Figure 2.
A More-O'Ferrall Jencks diagram illustrating the range of transition states possible for phosphate ester hydrolysis.

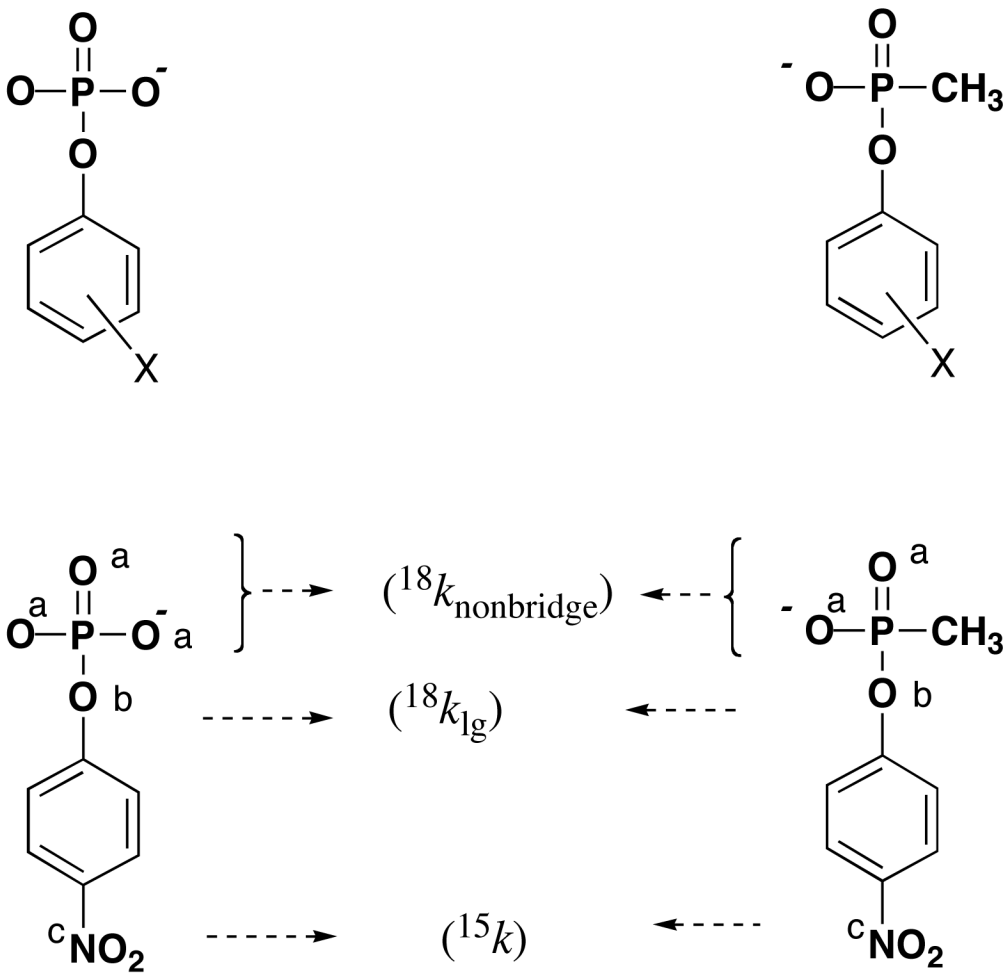

Figure 3.

Top, esters used for LFER experiments (X substituents are identified in Table 4). Bottom, the substrates *p*-nitrophenyl phosphate (4NPP) and *p*-nitrophenyl methylphosphonate (4NPMP) with the positions indicated at which isotope effects were measured. 4NPMP has two, and 4NPP has three nonbridging oxygen atoms (marked a). The scissile (leaving group) oxygen atoms are indicated by b, and the nitrogen atoms for ^{15}N KIEs are marked c.

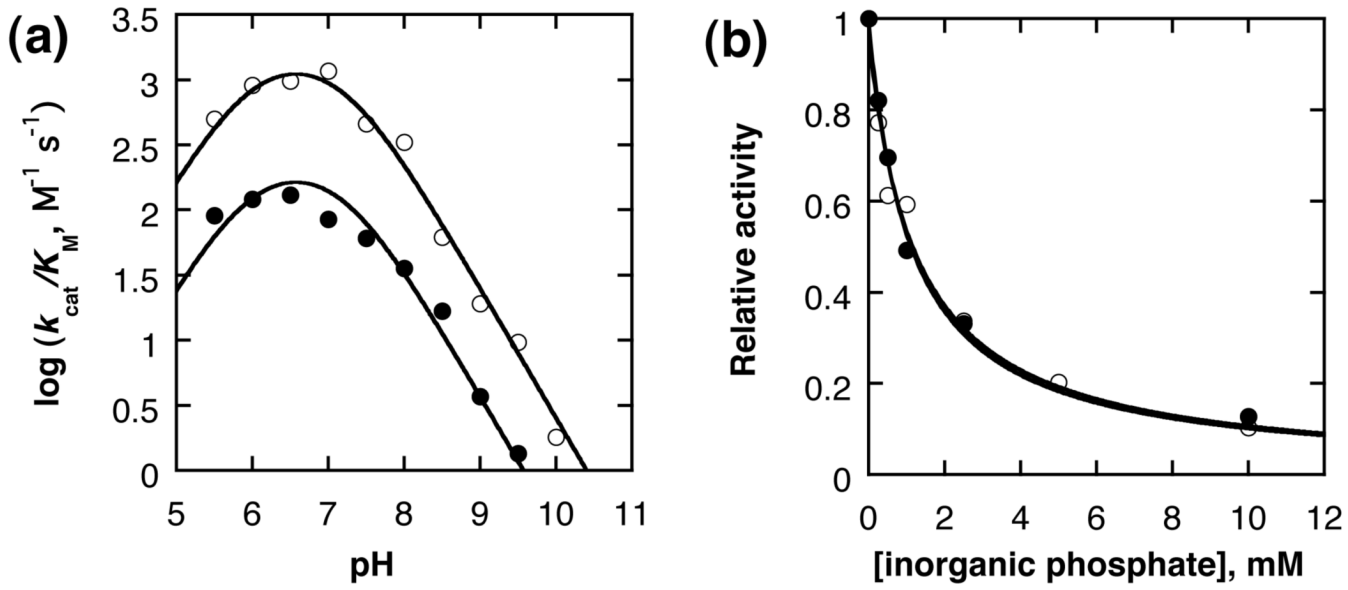

Figure 4.

(**a**) dependence of k_{cat}/K_M on pH for the hydrolysis of 4NPP (open circles) and 4NPMP (closed circles) catalyzed by PP1γ. Solid lines are fits to equation 1 as described in the text. (**b**) Inhibition by inorganic phosphate of 4NPP hydrolysis (open circles) and 4NPMP (closed circles) catalyzed by PP1γ at pH 8. Solid lines are fits to equation 2 as described in the text. Conditions: 25 °C, 100 mM buffer, 1 mM $MnCl_2$ (I = 0.45 M (NaCl)).

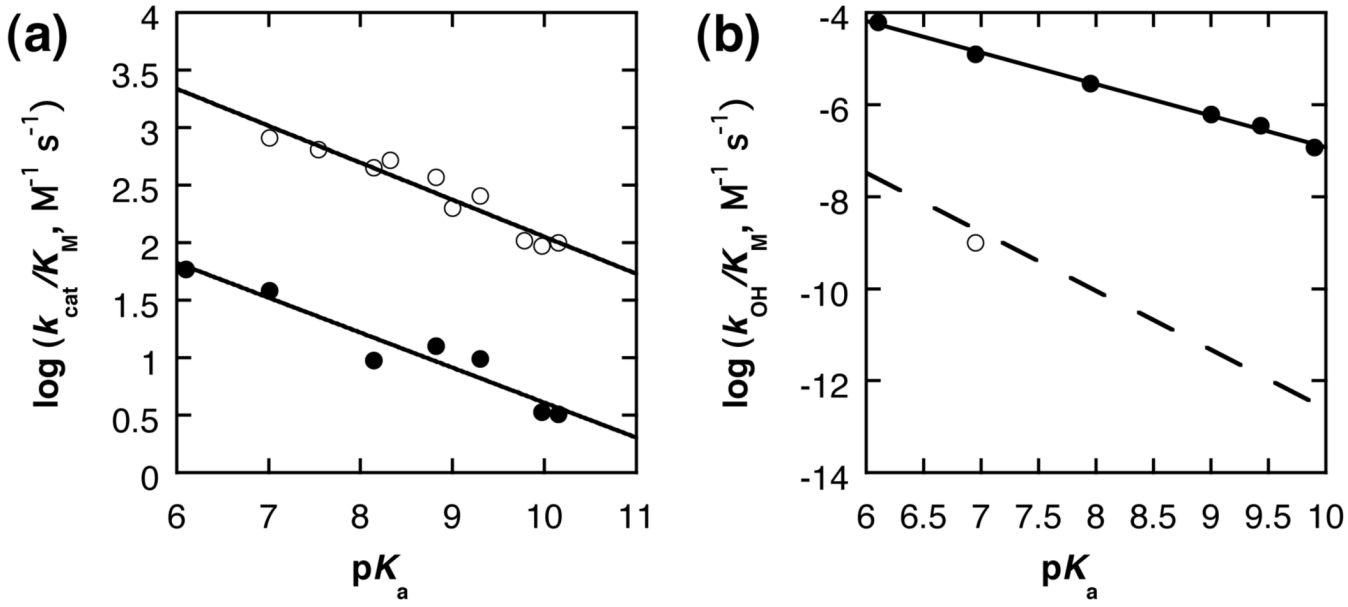

Figure 5.

(a) Brønsted plot for PP1γ catalyzed hydrolysis of aryl phosphates (open circles) and aryl methyl phosphonates (filled circles) (**b**) Brønsted plot for the base catalyzed hydrolysis of aryl methylphosphonates in solution (filled circles). The dotted line represents the best fit for the spontaneous hydrolysis of the dianions of phosphate monoesters (s^{-1})[8,21], and the open circle is the datum for the pH independent hydrolysis of 4NMP (s^{-1}) as reported in ref. [20].

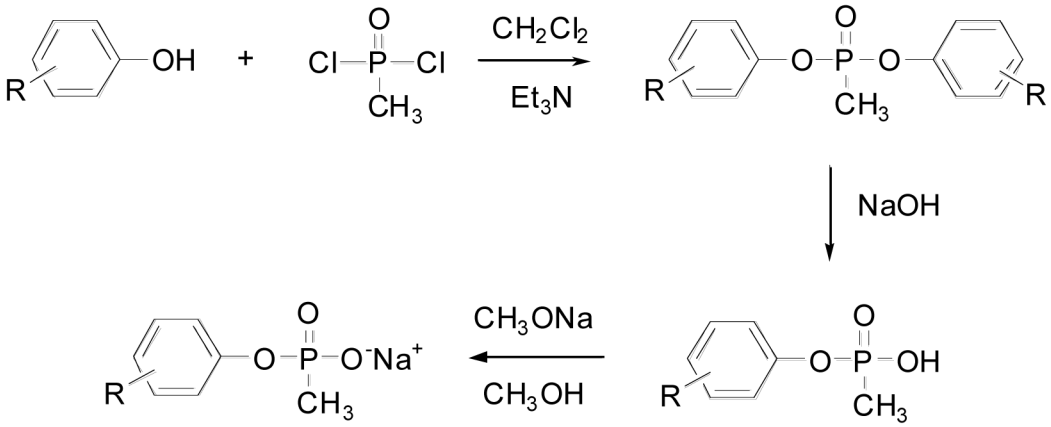

Scheme 1.

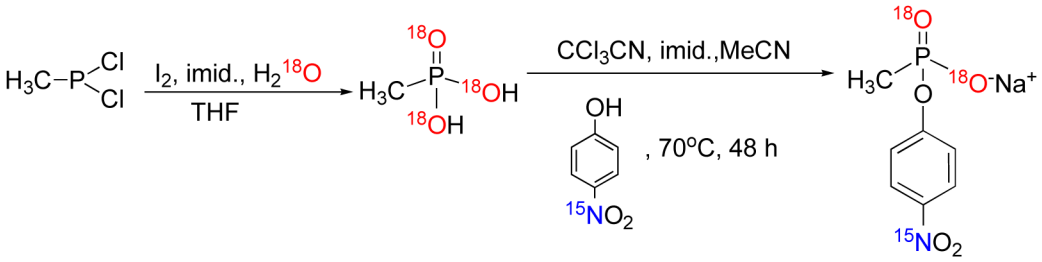

Scheme 2.

Table 1

Rate constants for PPlγ catalyzed hydrolysis of aryl phosphates and aryl methylphosphonates (25 °C, pH 8.0, 100 mM buffer (2-amino-2-methyl-1,3-propanedio), 1 mM $MnCl_2$, I = 0.45 M (NaCl)), and for the reaction of hydroxide with aryl methylphosphonates (25 °C, I=0.1M (NaCl)).

Aryl group	Phenol pK_a *(a)*	PP1γ-catalyzed phosphonate hydrolysis (k_{cat}/K_M, M^{-1} s^{-1})	PP1γ-catalyzed phosphonate hydrolysis (k_{cat}/K_M, M^{-1} s^{-1})	k_{HO}- catalyzed phosphonate hydrolysis (M^{-1} s^{-1})
4-nitro-3-fluoro	6.10	-	60±2	$6.2\pm0.2\times10^{-5}$
4-nitro	7.01	820±20	40±2	$1.18\pm0.01\times10^{-5}$
3-nitro-4-chloro	7.54	640±20	-	-
3-nitro	8.14	450±20	9.5±0.9	$2.9\pm0.2\times10^{-6}$ *(b)*
3,4-dichloro	8.32	520±50	-	-
3-chloro	8.82	370±10	12.6±0.7	$6.2\pm0.2\times10^{-7}$ *(b)*
3-fluoro	9.00	200±20	-	-
4-chloro	9.30	260±30	9.8±0.2	$3.6\pm0.4\times10^{-7}$ *(b)*
4-fluoro	9.78	104±17	-	
Phenol	9.97	94±12	3±1	$1.2\pm0.2\times10^{-7}$ *(b)*
4-methyl	10.15	100±3	3.2±0.2	

(a) pKas were measured by spectrophotometric titration at 25 °C

(b) extrapolated from measurements in 0.1 M NaOH at higher temperatures.

Table 2

KIE and LFER data for uncatalyzed and PP1-catalyzed reactions. The standard errors in the last decimal place are given in parentheses. The rate of the uncatalyzed reaction of the monoester required that these KIEs be measured at 95 °C. The faster rate of the phosphonate reaction with hydroxide permitted its hydrolysis to be performed at 25 °C. (a) These values are the range of KIEs reported for the reactions catalyzed by the native PTPs YopH,[26] VHR,[27] and PTP1.[26] (b) These values are the range of KIEs for reactions catalyzed by general acid mutants of the PTPs listed.

Results for reactions of *p*-nitrophenyl phosphate (4NPP)				
Isotope Effect	**Dianion H_2O attack, 95° C[28]**	**PP1-catalyzed**	**PTP-catalyzed[a]**	**PTP D to N mutant-catalyzed[b]**
$^{18}k_{nonbridge}$	0.9994 (5)	0.9959 (4)	0.9998-1.0003	1.0019-1.0024
$^{18}k_{nonbridge}$ per atom	0.9998 (5)	0.9986 (4)	0.9999-01.0001	1.00060-1.0008
$^{18}k_{nonbridge}$	1.0189(5)	1.0170(3)	1.0118-1.0152	1.0275-1.0297
^{15}k	1.0028(2)	1.0010(2)	0.9999-1.0001	1.0024-1.0030
β_{LG}	-1.23	-0.32	0.0 to -0.07[29]	

Results for reactions of *p*-nitrophenyl methylphosphonate (4NPMP)			
Isotope Effect	**Monoanion -OH attack, 25° C**	**PP1 -catalyzed**	**Range of values for hydrolysis of diesters[23]**
$^{18}k_{nonbridge}$	1.0015(4)	0.9973 (4)	1.0028-1.0056
$^{18}k_{nonbridge}$ per atom	1.0008(4)	0.9988 (4)	1.0014-1.0028
$^{18}k_{nonbridge}$	1.0098(4)	1.0129(3)	1.0042-1.0063
^{15}k	1.0006(3)	1.0010(1)	1.0007-1.0016
β_{LG}	-0.69	-0.30	